97-GT-459

MULTIVARIATE EXPERIMENTS TO ASSESS THE EFFECT OF COMBUSTOR DOME GEOMETRY ON FUEL DISTRIBUTION AND STABILITY

BREAK

**Leonel Arellano,[*] Arash Ateshkadi, Hirokazu Fukushima,
Vincent G. McDonell,[†] Scott Samuelsen[‡]**
University of California at Irvine
UCI Combustion Laboratory
Irvine, California 92697-3550

ABSTRACT

The geometric and operational features of gas turbine engine combustors are receiving increased scrutiny due to a growing concern regarding environmental impact, performance, durability, and manufacturability. To minimize the risk associated with new projects, optimization of designs which are similar to those in current operation is attractive. To achieve this goal, a methodology that is efficient and can reveal interactions between parameters that affect performance is necessary. An approach which addresses these requirements is statistically designed experiments (e.g., multivariate experiments or "design of experiments"), which offers efficiency as well as the ability to identify interactions between variables. This approach was adopted and demonstrated in the present study utilizing a set of hardware specifically developed to allow multivariate experiments to be conducted. A radial mixer geometry consisting of four parameters (primary and secondary swirl vane angles, the presence of a venturi, and the co-/counter swirl sense) was examined. The design was developed to maintain constant effective area and overall dimensions. The responses selected for study were stability (i.e., reaction lean blow-out) and fuel distribution.

The results reveal that (1) the multivariate approach is effective in the present application, (2) the swirl sense between the primary and secondary swirlers play an influential role in determining the uniformity of the spray, (3) the size of the fuel spray area is affected by the mixer venturi and the swirl sense, (4) the symmetry of the fuel presentation is affected by the interaction of the swirler angles, (5) Lean Blow Out (LBO) is not affected by the parameters selected, and (6) the parameters affecting fuel distribution and combustion stability differ, indicating that the combustion performance is not described entirely by fuel distribution.

NOMENCLATURE

A	Coded Factor for Primary Swirl Vane Angle	MS	Mean Square
ACd	Effective Area	n_{hi}	No. of experiments with parameter of high level
α	1-confidence level	n_{low}	No. of experiments with parameter of low level
B	Coded factor for secondary swirl vane angle	P	Percentage probability
C	Coded factor for swirl sense	RootMSE	Square root mean square error
CC	Counter-Swirl	SS	Sum of Squared deviations
Co	Co-Swirl	stdev	Standard deviation based on a sample
D	Coded factor for venturi	U	Uniformity Index
DF	Degrees of Freedom	U_s	Unmixedness
ΔP	Pressure drop (psi)	υ	Gray scale level
FN	Flow Number	$\bar{\upsilon}$	Average of gray scale levels in an image
i	Rank order	Y_{hi}	Response value associated with the high level of a parameter
LBO	Lean Blow-Out		
LSD	Least Significant Difference	Y_{low}	Response value associated with the low level of a parameter
m	Number of parameters		
$\dot{m}$	Fuel flow rate (lb/hr)	ϕ_{LBO}	Fuel/Air equivalence ratio at lean blow-out

[*] Student Member, ASME
[†] Member, ASME
[‡] Member, ASME, corresponding author (gss@uci.edu)

INTRODUCTION

To optimize the combustor performance of present day aircraft engines, attention is directed to combustor dome geometry. Fuel and air mixing hardware have been studied extensively in an attempt to develop an understanding of the processes leading to effective liquid fuel and air mixing, as well as, satisfactory combustion and emissions performances. For example, at the expense of time-consuming characterization via phase Doppler interferometry and CARS, it has been demonstrated that the performance of mixer hardware is sensitive to the geometry of its various components (Wang et. al, 1994a,1994b, 1995, Takahashi et. al, 1994). In addition, fuel/air mixing uniformity has been shown to play an important role in the combustion performance of direct liquid-fueled systems, pre-vaporized systems, as well as gaseous-fueled premixed systems (Pompei and Heywood, 1972, Lyons, 1982, Fric 1993). As instructive as this information is, the effects of geometry and hardware design have not been fully explored.

To address this issue, the present effort adopts a set of "radial dome hardware" designed to allow a systematic, statistically-based, multivariate study to be conducted. This protocol leads to an efficient identification of critical parameters (factors) associated with the process (response) of interest.

The responses selected to assess the effect of parametric variation on mixer performance are (1) fuel distribution (derived from non-reacting experiments), and (2) the equivalence ratio at lean blow-out (LBO, derived from reacting experiments).

Fuel distribution was selected as a response since it has been previously shown to be related to emissions performance, and it provides a basis for the development of more mechanistic descriptions of the processes occurring. Fuel distribution was assessed utilizing Planar Laser Liquid-Induced Fluorescence (PLLIF) in a time-efficient, non-intrusive manner.

LBO was selected as a response to (1) reflect the general narrowing of stability limits associated with advanced emissions control technologies, and (2) to provide an efficient assessment of combustion performance.

The approach followed in the present research was to (1) construct a statistically-sound matrix of experiments through Design of Experiments, (2) apply PLLIF in a non-reacting environment to characterize the effect of hardware geometry variations on fuel distribution, (3) assess the effect of hardware geometry variations on LBO in a reacting environment, and (4) develop relationships between hardware parameters and both fuel distribution and LBO.

EXPERIMENT
Hardware

The mixer hardware utilized provides geometric variations of the elements labeled in Figure 1, within the ranges identified in Table 1. A key strategy (and challenge) in the experimental design was to maintain (1) the total effective area of the mixer constant for any of the configurations possible (to manufacturing tolerances), and (2) the effective area of each swirler constant. The secondary swirlers were designed to account for about 60% of the total effective area of the mixer and the primary swirlers to account for about 40%.

All the experiments were conducted with a simplex pressure atomizer with flow number of 1.5* and an included spray angle of 90°.

Table 1. Test Parameters and Ranges Examined

Parameters	Levels
Primary Swirl Vane Angle	25°, 35°, 45°
Secondary Swirl Vane Angle	55°, 65°, 75°
Swirl Sense	Co-Swirl, Counter-Swirl
Venturi	Present, Not Present

Facilities

The facility employed for the non-reacting studies consisted of a 76.2 mm inner diameter plenum through which air was supplied to the mixer. A 6.35 mm tube running inside the plenum supplied liquid fuel to the fuel nozzle assembled with the mixer (Figure 1). The configuration was oriented vertically, and fuel was sprayed downwards in an unconfined fashion (Figure 2).

The facility utilized for the reacting studies was similar to that employed for the non-reacting experiments, but featured an up-fired arrangement. An 80 mm quartz tube served as the combustor liner allowing for superior visualization of reactions. The liner was 2.5 liner diameters in length, and provided an area contraction at the exit of 60% to provide some back-pressure.

Operating Conditions

Non-reacting. Liquid methanol served as the fuel in the non-reacting fuel distribution studies. Liquid methanol allowed fluorescein dye to be utilized with an Argon-ion Planar Laser Liquid-Induced Fluorescence (PLLIF) system. In each case, air flow-rates to induce a 4% pressure drop relative to the downstream pressure (101 kPa) were maintained across the radial mixer hardware. This corresponded to air flow rates of about 53 kg/hr for a baseline operating equivalence ratio of 0.7 (about 6 kg/hr methanol). The air and fuel employed were at a temperature of 20-25° C.

Reacting. All reacting experiments used liquid Jet-A and air at room temperature. The experiments were conducted in an up-fired arrangement (described above) at atmospheric conditions. As in the non-reacting experiments, air flow rates to maintain a 4% pressure drop were sustained.

Measurement Protocol

Fuel Distribution. Planar Laser Liquid-Induced Fluorescence (PLLIF) was employed to characterize the planar distribution of fuel dnwnstream of the mixer. In the setup utilized, a laser sheet passed through the fuel spray at a distance equivalent to one (mixer) flare diameter (25.4 mm) downstream (Figure 2). The laser energy induced fluorescence from fluorescein molecules doped in the liquid fuel, which in turn was proportional to the fuel mass (Igushi et. Al, 1993). An Ar⁺ laser operating at a wavelength of 0.4880 mm was used to generate a laser sheet, and gray scale images of the spray were

---

* $FN = \dfrac{\dot{m}}{\sqrt{\Delta P}}$, where $\dot{m}$ is the fuel flow rate (lb/hr) and ΔP is the pressure drop across the injector (psi)

generate a laser sheet, and gray scale images of the spray were captured on a computer using an intensified CCD camera. A total of 32 images of the fuel spray were captured and averaged for the analyses conducted. Being a planar imaging technique, PLLIF was relatively quick to apply to assess the distribution of fuel in the spray.

Gray scale images captured on computer via the PLLIF system were analyzed to determine (1) the area occupied by the fuel spray, (2) the uniformity of the fuel spray, and (3) the distribution of fuel.

A value that quantifies the degree of liquid fuel and air mixing was employed and based on the "Unmixedness" parameter (Dankwertz, 1952). In the present case, a Uniformity Index (U) value was defined as: the ratio of the standard deviation of the gray scale levels captured with the CCD camera to the average gray scale level obtained in the image.

$$U = \frac{stdev(\upsilon)}{\bar{\upsilon}}. \qquad (1)$$

The lower the Uniformity Index (U) calculated, the more uniform the distribution of fuel is in the spray. The attractive feature of defining U this way is that the intensity setting of the camera becomes irrelevant when dividing the standard deviation by the average value of gray scales (not the case in other methods that calculate "unmixedness") (Fukushima, 1996). Hence, the values for assessing the degree of fuel and air mixing (via U) are independent of the camera gain setting used to acquire the image.

Lean Blow Off. The stability of reactions was evaluated by recording the equivalence ratio at which lean blow-out occurred. Fuel and air flow rate data were recorded on computer (real time) via a data acquisition system. Lean blow-out was induced by reducing the fuel flow rate and maintaining a fixed air pressure drop across the mixer.

Multivariate Experimentation

A powerful experimental tool with which to study multiple variables is through statistical "multivariate experiments" or "statistically designed experiments" (Fisher, 1935). Although these techniques have existed for some time, renewed industrial interest in quality control and process optimization through these tools has been brought about by the notoriety gained by Taguchi methods. In the 1980's, Taguchi revealed an innovative approach for reducing variation in products and processes while demonstrating the utility of statistical tools (Taguchi, 1987). These methods, and other statistically based experimentation approaches, have been made accessible to engineers through advancement of computational resources. With graphical user interfaces and improved computing power, software now provide a straight-forward connection between engineering scientist and the complex analysis techniques and statistical methods (Design-Ease 3, 1995).

Design of Experiments (DOE) was employed to develop a matrix of 20 experiments for investigating the role of geometrical parameters on mixer performance. With no prior knowledge of the role hardware parameters played on any response, a screening design was selected rather than an optimization design. As a result, a "full factorial," two-level screening design was used to study the four parameters listed in Table 1. Center-points (intermediate values/levels of parameters) were

included to evaluate curvature in the responses. The experiments were conducted randomly to minimize the effects of uncontrolled parameters (Table 2). The matrix of experiments followed reduced variability and bias that would be generated by a "methodical approach" (the strategy of varying one parameter at a time). In addition, a methodical approach would not identify combined effects of parameters involved—crucial in any parametric study (Box et. al, 1978). Attractive was also the fact that, with a factorial approach, Analysis of Variance (ANOVA) for the response data acquired could directly lead to mathematical relations between response and (hardware) parameters.

RESULTS AND DISCUSSION

The results of measurements conducted to assess the variation of mixer effective area are presented first, and the results associated with the statistically-designed experiment follow.

Radial Mixer Effective Area

Each hardware configuration in the test matrix was tested to assess the variation of effective area (ACd) among different configurations. The hardware configurations were defined according to (1) the primary swirler used, (2) the secondary swirler employed, (3) the relative swirl sense, and (4) the use of a venturi. The pressure drop across the mixer was maintained constant at 4% and the measured mass flow-rate of the air served to define ACd. Figure 3 illustrates results of the effective area for the 20 hardware configurations tested. The average effective area was 145.5 mm^2 with the maximum measured value varying by 13.4% and the minimum value varying by 12.6%.

Factorial Study

Table 2 lists the mixer configurations experimented with under reacting and non-reacting conditions. This matrix of experiments represents a full factorial design as explained above. All the responses obtained (uniformity, spray area, spray symmetry, LBO) were analyzed using analysis of variance (ANOVA). To illustrate the protocol, some details of the analysis are provided for the Uniformity Index (U) section below.

Table 2. Full Factorial Study

Run Number	Factor A Primary S Angle	Factor B Secondary S Angle	Factor C Swirl Sense	Factor D Venturi
1	25	75	CC Counter-Swirl	W/O
2	25	75	CC Counter-Swirl	W
3	45	55	CC Counter-Swirl	W
4	25	75	CO Co-Swirl	W
5	35	65	CO Co-Swirl	W/O
6	45	55	CO Co-Swirl	W/O
7	45	75	CC Counter-Swirl	W
8	45	55	CC Counter-Swirl	W/O
9	35	65	CC Counter-Swirl	W
10	25	75	CO Co-Swirl	W/O
11	45	75	CC Counter-Swirl	W/O
12	25	55	CC Counter-Swirl	W/O
13	35	65	CO Co-Swirl	W
14	45	75	CO Co-Swirl	W
15	45	75	CO Co-Swirl	W/O
16	35	65	CC Counter-Swirl	W/O
17	25	55	CO Co-Swirl	W
18	45	55	CO Co-Swirl	W
19	25	55	CO Co-Swirl	W/O
20	25	55	CC Counter-Swirl	W

Uniformity Index (U)

To isolate the effect a parameter (or a combination of parameters) has on a response, it is necessary to know how the response varies as the parameter varies from its low level to its high level. To assess this variation (or *Effect*), all the responses corresponding to a configuration employing the low and high levels are averaged, and their difference is taken. That is,

$$Effect = \frac{\sum Y_{hi}}{n_{hi}} - \frac{\sum Y_{low}}{n_{low}}, \qquad (2)$$

where Y_{hi} is the response value associated with the high level of a parameter (or combination of parameters), Y_{low} is that associated with the low level, n_{hi} is the number of experiments employing the high level, and n_{low} is the number using the low level (Box et. al, 1978). *Effects* calculated for the Uniformity Index (U) response are listed in Table 3.

Table 3. The *Effects* on The Uniformity Index (U)

Run Number	Unmixedness Us	Factor or Factor Interaction	Effect on Unmixedness
1	0.2373	A	0.0208
2	0.2491	B	0.0146
3	0.2333	C	-0.0509
4	0.2693	D	-0.0052
5	0.2743	AB	-0.0045
6	0.3005	AC	-0.0116
7	0.2394	AD	0.0220
8	0.2320	BC	0.0052
9	0.2358	BD	0.0162
10	0.2712	CD	-0.0088
11	0.2595	ABC	0.0015
12	0.1975	ABD	-0.0018
13	0.2895	ACD	-0.0029
14	0.2712	BCD	-0.0024
15	0.3221	ABCD	-0.0013
16	0.2116	A - Primary Swirler	
17	0.2728	B - Secondary Swirler	
18	0.2859	C - Swirl Sense	
19	0.2368	D - Venturi	
20	0.2432		

Through the Central Limit Theorem, it is expected that as a sample size increases, the distribution of averages becomes normal. Hence, if the *Effects* on a response by hardware parameters (or combinations of parameters) are truly random, their distribution will be normal. To explore any deviation from this, a probability plot can be generated for the *Effects* on responses (Box et. al, 1978). Figure 4a shows the normal probability plot of the effects calculated for the Uniformity Index (U). The percentage probability is determined from

$$P = \frac{100}{m}\left(i - \frac{1}{2}\right), \qquad (3)$$

where m is the number of parameters and combinations of parameters, and i is the rank order. As seen in Figure 4a the effect caused by the swirl sense deviates significantly from a normal distribution (hence, its effect is not random). The deviation signifies that swirl sense plays a strong role in determining spray uniformity (U) in the configurations tested. Figure 4b illustrates how the averaged values of configurations

employing Co-Swirl (CO) and Counter-Swirl (CC) vary. In general, U decreases (spray fuel uniformity increases) when the swirlers act in opposite directions. The PLLIF images of the configuration resulting in the lowest U (Configuration 12 employing CC-Swirl) and the highest U (Configuration 15 employing Co-Swirl) are shown in Figures 5a and 5b.

The significance of explaining U with swirl sense can be assessed by applying the statistical F-test. The F value may be computed from the ratio of the Mean Square of the model (MS_{model}) and the Mean Square of the residuals ($MS_{residuals}$) (Design-Ease 3, 1995, Box et. al, 1978). Or,

$$F = \frac{MS_{model}}{MS_{residuals}} = \frac{\left(SS_{model}/DF_{model}\right)}{\left(SS_{residuals}/DF_{residuals}\right)}, \qquad (4)$$

where SS represents the Sum of Squared deviations, and DF is the Degrees of Freedom. SS can be obtained from

$$SS = \frac{N}{4}\left(Effect^2\right). \qquad (5)$$

For this case, swirl sense is the only parameter identified ($DF_{model} = 1$), and it has a Sum of Squared deviations of 0.0103 (refer to Table 3 for the C *Effect*). The residuals yield $SS_{residuals} = 0.0073$ with $DF_{residuals} = 17$. The resulting F value is about 24 ($\gg 1$). As can be verified from a chart of Percentage Points of the F Distribution, this F value indicates that swirl sense can in deed be used to explain the Uniformity Index (U) with 99% confidence.

Spray Area

The spray cross-sectional area was measured at an axial plane of one-flare diameter (25.4 mm) downstream from the mixer exit. The same statistical procedures outlined in the previous section were employed to interpret the results. An Analysis of Variance (ANOVA) reveals that (1) the presence of the venturi and (2) the swirl sense play strong roles in determining the size of the spray area. The swirl sense and the venturi effects showed deviation from the normal probability distribution (Figure 6a). As detailed above, the deviation from the normal distribution points to the fact that the factors associated play a role in skewing the response (area of the spray) in a certain direction.

Closer observation of the data reveals that in general (1) the spray area is smaller when the venturi is present or when the swirlers act in opposite directions (Counter-Swirl), and (2) the spray area is larger when the venturi is not present and the swirlers act in the same direction (Co-Swirl). These trends are illustrated in Figures 7a and 7b by the average area of the spray resulting from configurations of interest. Figure 8a illustrates the PLLIF image of the spray for Configuration 15, which employed a Co-Swirl arrangement without a venturi. The large spray generated is explained by (1) the increased swirl strength induced when the primary and secondary swirlers act in the same direction, and (2) the absence of the venturi which when present will physically block the fuel spray and reduced the area downstream. Figure 8b is a PLLIF image for Configuration 20, which consisted of a Counter-Swirl (weaker resultant swirl) arrangement and a venturi (physical blockage of fuel), hence resulting in small spray area.

It is noteworthy that the interaction of the swirl sense and the venturi (CD) was not identified as a main effect (did not deviate from

4

the normal distribution) (Figure 6a). However, comparing the average spray areas observed for configurations as shown in Figure 6b reveals that Co-Swirl tends to increase the area more drastically when the venturi is not employed. The means of the two factors can be compared better by assessing the Least Significant Difference (LSD) with a selected confidence level for a t-distribution (Design-Ease 3, Box et. al, 1978). That is, the Least Significant Difference between the two averages should be

$$LSD = \overline{Y_i} - \overline{Y_j} = t_{\alpha/2,OF} \, RootMSE \sqrt{\frac{2}{n}} \, . \qquad (6)$$

For 95% confidence ($\alpha = 0.05$) that the difference is significant, and 19 degrees of freedom, a t-distribution gives $t = 2.093$ (Box et. al, 1978). Therefore, the least required difference LSD = 1700 mm². On Figure 6b this value is plotted as a bar in between the averages. As can be seen, only the comparison of configurations not utilizing a venturi with Co-Swirl versus Counter-Swirl may be made with confidence (the difference between means is greater than the least required); which is not surprising since the interaction of swirl sense and venturi (CD) was not identified as a main effect (Figure 6a).

Spray Symmetry

Symmetry of the spray was assessed by comparing the distance between the center of mass of the spray (gray scale levels from the PLLIF images are directly related to mass of liquid), and the geometric center of spray area (centroid). The interaction of the swirler angles (Primary and Secondary Swirlers) was the only main effect identified from a deviation of the expected normal distribution (Figure 9a). Even then, the symmetry of the spray is affected the most when the secondary swirler angle is maintained small (55°), and the primary swirler angle is allowed to change (Figure 9b). As shown on Figure 9b, when the secondary swirl angle is small, the primary swirl angle plays an important role in the symmetry with strong Co-swirl leading to worse symmetry. However, when the secondary swirl is large, the primary swirl angle does not play a significant role (Figure 9b).

LBO

The equivalence ratio at which Lean Blow Out (LBO) occurred was not dominated by any mixer parameters or their interactions in the experiments conducted. All the Effects calculated followed a normal distribution closely (Figure 10). Such information points to the fact that other parameters (not included in the matrix of experiments) dominate LBO significantly more than mixer parameters at the operating conditions tested. It is suspected that different reaction stability mechanisms evolved due to recirculation zone characteristics that may, or may not have changed drastically with the variation of mixer hardware. Furthermore, different stability mechanisms may have interacted, or may have been affected by interactions of parameters un-accounted for in this study. Considering these possibilities, it can be speculated that under different operating conditions results may tell a different story; including one where mixer parameters are important.

LBO and Fuel Distribution

A correlation between the non-reacting fuel distribution characteristics and the equivalence ratio at LBO was not revealed with this research. In a previous study with a similar (but not identical) fuel

injection scheme, a one-to-one relationship between unmixedness and LBO was established (McDonell, 1996). In the previous study, the size/strength of the recirculation zone was maintained constant for all the configurations tested. It is suspected that, in that case, the controlling stability mechanism remained the same and thereby allowed for the direct study of a mixer parameter (fuel nozzle alignment) on LBO. In the present case the mechanism or mechanisms controlling stability (LBO) may have varied in an uncontrolled fashion, thus removing their effect from the analysis.

SUMMARY AND CONCLUSIONS

A statistically-based (factorial) study of the effect of mixer geometry on the non-reacting spray structure and combustion stability for a radial mixer assembly was conducted. Planar Laser Liquid-Induced Fluorescence (PLLIF) was employed for the non-reacting assessment, and the equivalence ratio at Lean Blow-Out (LBO) was utilized to characterize stability of the combustion process. The study demonstrated that:

- Multivariate experiments, designed and analyzed by statistically-based methods, can provide an effective strategy to reveal the sensitivity of combustor performance on hardware design in a complex dome system.
- The Uniformity (*U*) of the spray is strongly determined by the *swirl sense* of the two swirlers composing the mixer (Primary Swirler and Secondary Swirler). In general, the uniformity of the fuel spray improves when the swirlers act in opposite direction. The angle of the swirlers does not affect uniformity as significantly as swirl sense.
- The size of the spray area is determined primarily by the mixer venturi and the swirl sense. The spray area is reduced when the venturi is present or when the swirlers act in opposite directions, and the spray area is enhanced when the venturi is not present or the swirlers act in the same direction. The mixer venturi can physically block the fuel spray trajectory and reduced the area of the spray.
- The symmetry of the fuel presentation is affected by the interaction of the swirler angles. The symmetry of the spray is affected the most when the secondary swirler is maintained small and the primary swirler angle is allowed to change. The spray is more symmetric when both, the primary and secondary swirlers, have small angles. The symmetry is the worst when a small secondary swirler angle is used in conjunction with a large primary swirler angle.
- LBO is not dominated by any of the mixer parameters studied (or interaction of mixer parameters) under atmospheric tests employing fuel and air at ambient temperature, and an 80 mm combustor liner of 2.5 L/D with 60% area contraction at the exit. This reveals that a parameter(s) not explicitly studied is/are important in determining stability under such operating conditions.
- The parameters affecting fuel distribution characteristics and combustion stability do not correlate, indicating that the LBO is not described entirely by fuel distribution in the present case and that the factors affecting LBO were not accounted for in the test matrix.

REFERENCES

Box, G. E. P., Hunter, W. G., and Hunter, J. S., 1978, *Statistics for Experimenters: An Introduction to Design, Data analysis, and Model Building*, New York, Wiley & Sons.

Dankwertz, P.V, 1952, "The Definition and Measurement of Some Characteristics of Mixtures," *Applied Scientific Research., Section A, Vol.* 3, pp. 279-296.

Design-Ease 3, 1995, Computer Software, Stat-Ease Inc., Minneapolis, Minnesota, IBM-PC.

Fisher, R.A., 1935, *The Design of Experiments*, Edinburgh, London, Oliver and Boyd.

Fric, T., 1993, "Effects of Fuel-Air Unmixedness on NOx Emissions," *Journal of Propulsion and Power*, Vol. 9, pp. 708-713.

Fukushima, H, McDonell, V.G., and Samuelsen, G.S., 1996, "Assessment of Potential Tools to Describe Mixing Characteristics of Liquid Fuel," submitted to *Applied Optics*.

Igushi, T., McDonell, V.G., and Samuelsen, G.S., 1993, "An Imaging System for Characterization of Liquid Volume Distributions in Sprays," *Proceedings, 6th annual ILASS-Americas Conference*, submitted to *Atomization and Sprays*.

Lyons, V.J., 1982, "Fuel/Air Nonuniformity—Effect on Nitric Oxide Emissions," *AIAA Journal*, Vol. 20, pp. 660-665.

McDonell, V.G., Arellano, L., Lee, S.W., and Samuelsen, G.S., 1996, "Effect of Hardware Alignment on Fuel Distribution and Combustion Performance for a Production Engine Fuel-Injection Assembly," In press, *26th Symposium (International) on Combustion*, The Combustion Institute, Pittsburgh.

Pompei, F. and Heywood, J.B., 1972, "The Role of Mixing in Burner Generated Carbon Monoxide and Nitric Oxide," *Combustion and Flame*, Vol. 19, pp. 407-418.

Taguchi, G., 1987, *System of Experimental Design: Engineering Methods to Optimize Quality and Minimize Cost*, New York, UNIPUB/Kraus International.

Takahashi, F., Schmoll, J., Switzer, G.L., and Shouse, D.T., 1994 "Structure of a Spray Flame Stabilized on a Production Engine Combustor Swirl Cup," *Twenty-Fifth Symposium (International) on Combustion*, The Combustion Institute, Pittsburgh, pp. 183-191.

Wang, H.Y., McDonell, V.G., and Samuelsen, G.S., 1994a, "Experimental Study of a Model Gas Turbine Combustor Swirl Cup 1—2-Phase Characterization," *Journal of Propulsion and Power*, Vol. 10, pp. 441-445.

Wang, H.Y., McDonell, V.G., and Samuelsen, G.S., 1994b, "Experimental Study of a Model Gas Turbine Combustor Swirl Cup 2—Droplet Dynamics," *Journal of Propulsion and Power*, Vol. 10, pp. 446-452.

Wang, H.Y., McDonell, V.G., and Samuelsen, G.S., 1995, "Influence of Hardware Design on the Flow Field Structures and the Patterns of Droplet Dispersion" *Journal of Engineering for Gas Turbines and Power—Transactions of the ASME*, Vol. 117, pp. 282-289.
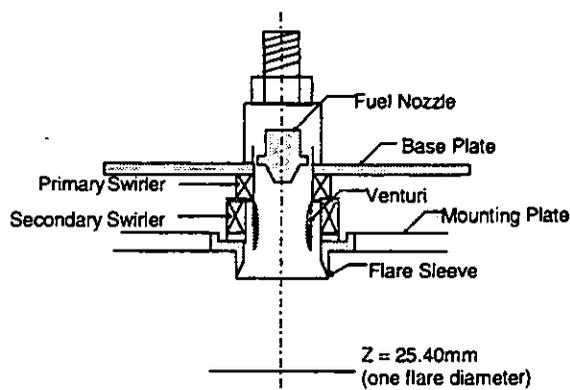
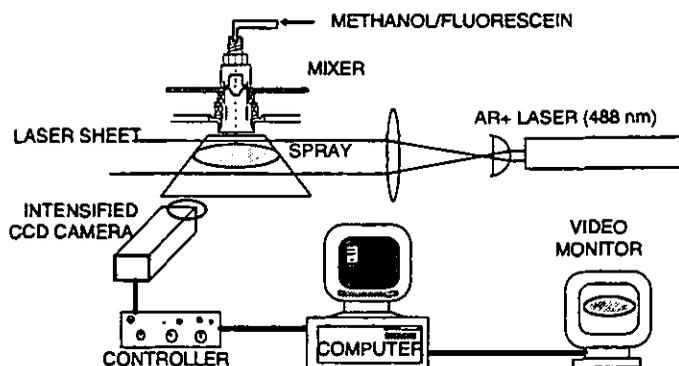**Figure 1. Schematic of the Generic Radial Mixer Assembly**

Figure 2. PLLIF and Non-reacting Experiment Setup
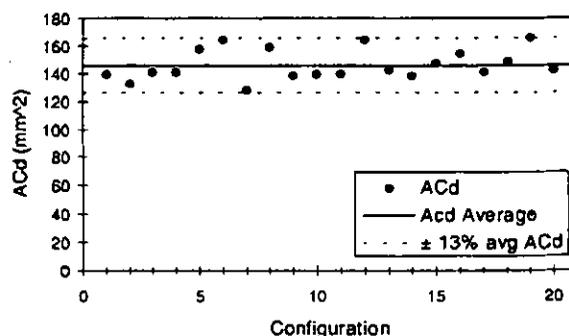

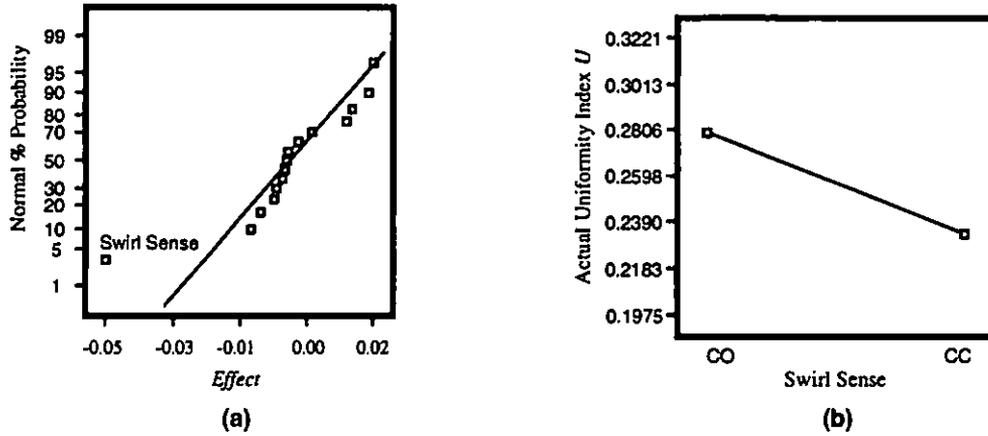**Figure 3. Effective Areas (ACd) for Each Hardware Configuration**

6

Figure 4. (a) Probability Plot for Uniformity Index Response, (b) Effect of Swirl Sense on Uniformity Index Response
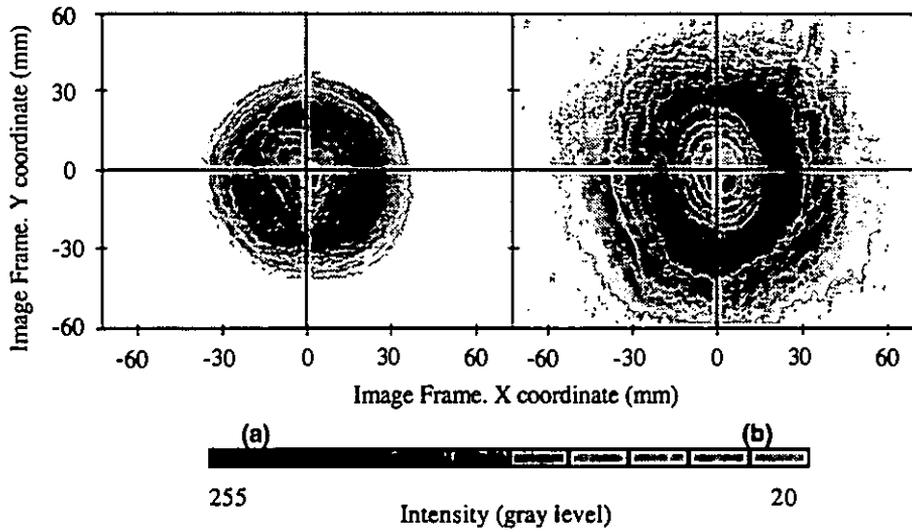

**Figure 5. PLLIF Images of Spray Taken at One Flare Diameter Downstream:
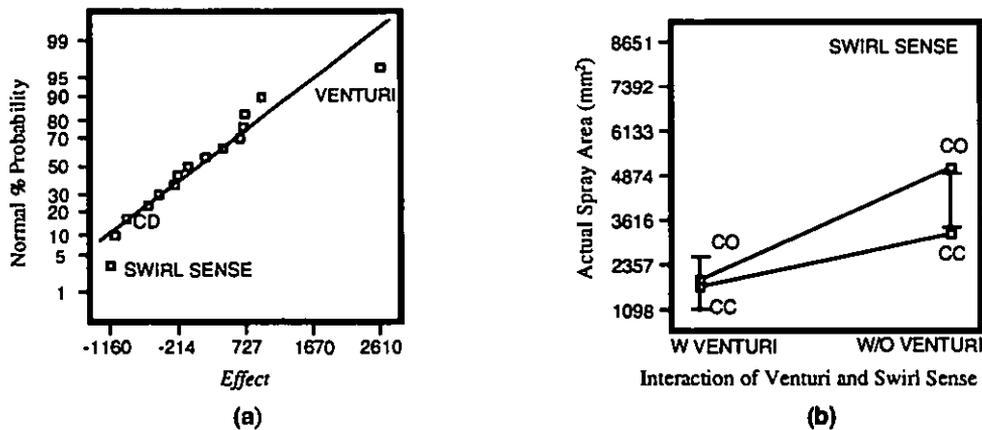(a) Configuration 12 (Counter-Swirl) (b) Configuration 15 (Co-Swirl)**

**Figure 6. (a) Normal Probability Plot for Effects on Spray Area
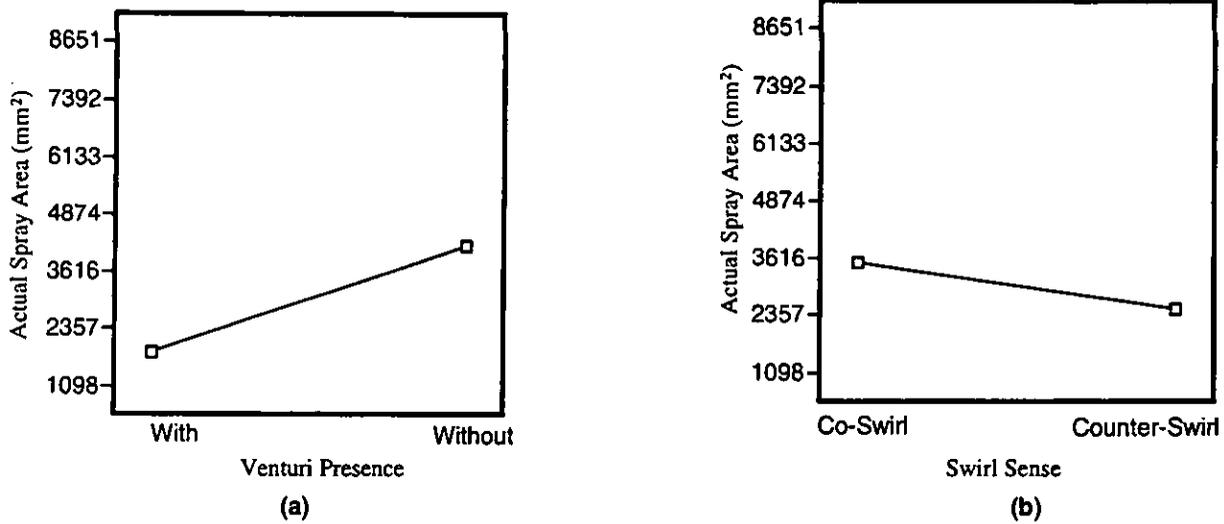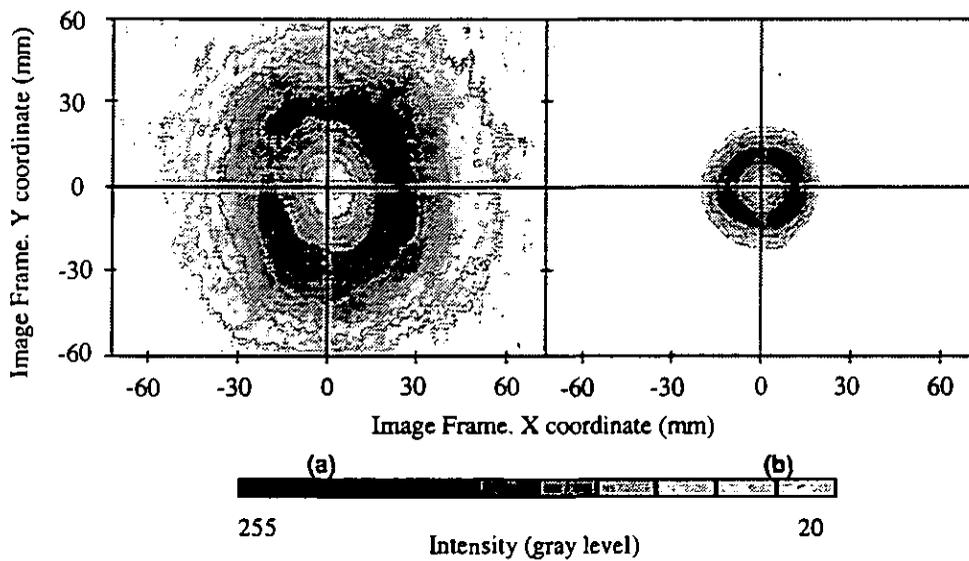(b) Average Trends of Spray Area as a Function of Venturi and Swirl Sense**

7

Figure 7. Main Effect of Hardware Parameters on Spray Area: (a) Effect of Venturi,
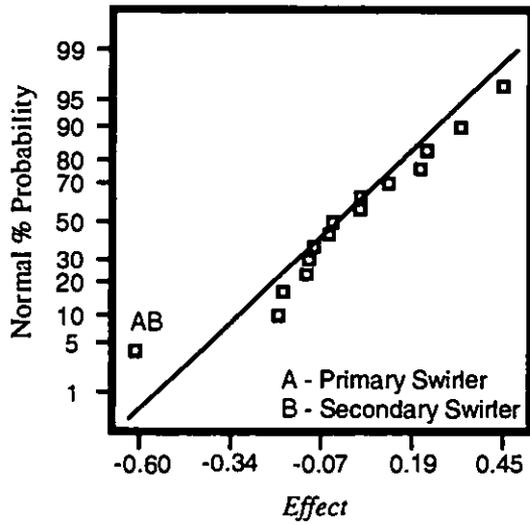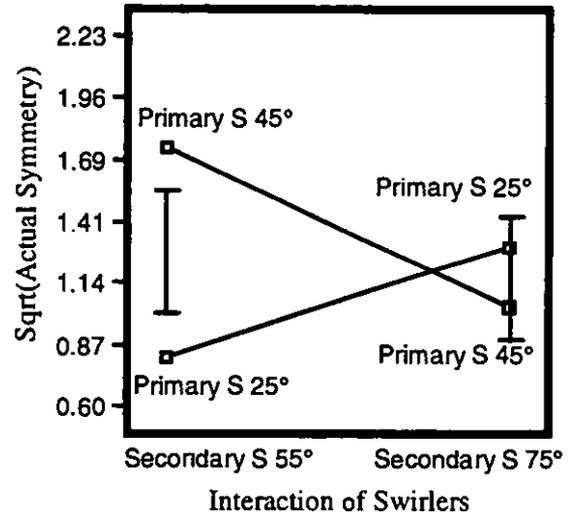
(b) Effect of Swirl Sense

Figure 8. PLLIF Images of Spray Taken at One Flare Diameter Downstream:
(a) Configuration 15 (Co-Swirl, w/o Venturi), (b) Configuration 20 (CC-Swirl, w/ Venturi)

(a)	(b)

Figure 9. **(a) Normal Probability Plot for Effects on Spray Symmetry (b) Average Trends of Spray Symmetry as a Function of Primary and Secondary Swirler Angles**
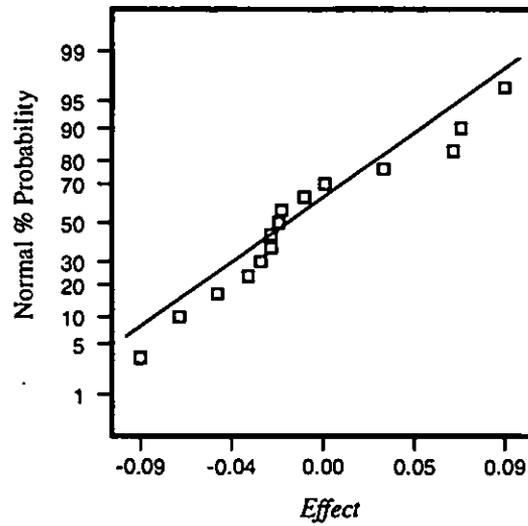

Figure 10. Normal Probability Plot for Effects on Equivalence Ratio at LBO

9